Quantum magnetoresistance in the Ca-intercalated graphite superconductor CaC_6

Gang Mu,[1,*] Qiucheng Ji,[1] Wei Li,[1,2,†] Xuguang Xu,[1] Tao Hu,[1] Da Jiang,[1] Zhi Wang,[3] Bo Gao,[1] Xiaoming Xie,[1] and Mianheng Jiang[1]

[1]*State Key Laboratory of Functional Materials for Informatics and Shanghai Center for Superconductivity, Shanghai Institute of Microsystem and Information Technology, Chinese Academy of Sciences, Shanghai 200050, China*

[2]*State Key Laboratory of Surface Physics and Department of Physics, Fudan University, Shanghai 200433, China*

[3]*School of Physics and Engineering, Sun Yat-Sen University, Guangzhou 510275, China*

(Received 27 July 2014; revised manuscript received 18 November 2014; published 29 December 2014)

The search for exotic materials with a linear Dirac-like dispersion in the electronic structure is one of the most challenging tasks of the condensed matter community and materials science. Revealing the nature of the interplay between such a Dirac-like and superconducting states is a crucial issue for the study of fundamental physics. Here we report the experimental observations of a large linear magnetoresistance (MR) in the Ca-intercalated graphite superconductor CaC_6. A large nonsaturating MR with a magnitude as high as 244% is observed at low temperature under a magnetic field of 9 T. The magnetic field (B) dependence of MR shows a linear behavior above 3 T at low temperature, which deviates from the classical B^2 behavior, pointing to the existence of an intrinsic linear Dirac-like state. The presence of such a low-energy Dirac-like dispersion in energy band structure is confirmed qualitatively by performing first-principles calculations. These findings may pave an avenue for potential applications in magnetoelectronic sensors and for further studying the interplay between the linear Dirac-like and superconducting states in exotic materials.

DOI: 10.1103/PhysRevB.90.214522 PACS number(s): 74.70.Wz, 75.47.−m, 71.70.Di, 74.25.Jb

I. INTRODUCTION

In this decade the study of Dirac-like states in materials has triggered great research interests in both the condensed matter community and materials science. These states have been found in two dimensions in graphene [1], on the surfaces of topological insulators [2,3] and Weyl semimetals [4,5], as well as in the three-dimensional bulk states of the parent compound of iron-based superconductor $BaFe_2As_2$ [6]. Due to the presence of the linear relation between momentum and energy in these materials, an anomalous large linear quantum magnetoresistance (MR) has been observed in transport measurements [7–13], in contrast to the case of conventional materials where a variation as a function of B^2 is expected [14]. This is interpreted as the quantum limit by Abrikosov where only the lowest Landau level is occupied because of the larger Landau level spacing near the Dirac points [15,16]. Such a condition is usually difficult to achieve because a very high magnetic field beyond the laboratory range is needed. Due to the larger Landau level spacing near the Dirac points, however, a magnetic field of several teslas can satisfy this requirement if the system has a linear Dirac-like dispersion [1]. However, serval recent experimental and theoretical results indicate that the linear MR can be observed in systems with electrons occupying up to high Landau levels [11,13,17,18]. This suggests that Abrikosov's theory can be generalized to high Landau levels. Furthermore, the extrinsic effects, such as sample inhomogeneity [19] and/or the disorder-induced quantum interference effect [20,21], may also contribute to such an anomalous linear MR. The benefit of realizing large MR has potential applications in magnetoelectronic sensors. From the viewpoint of fundamental physics, the Dirac-like states can coexist with superconductivity leading to the emergence of exotic electronic states and physical phenomena in condensed matter [22,23].

Recently, one of the present authors has co-worked on a report on the quantum MR in underdoped superconductor $Ba(Fe_{1-x}Ru_xAs)_2$ [8], which vanishes gradually with the increase of Ru concentration. In order to explore the unusual linear quantum MR in pure superconductors, we focus both experimental and theoretical attention on the intercalated graphite superconductor CaC_6, which has been successfully synthesized and reported to be a superconductor with critical transition temperature $T_c \sim 11.5$ K in 2005 [24,25]. The T_c of CaC_6 can be raised to 12.3 K by applying an external pressure of 16 kbar [26]. Compared to pure graphite, the electronic structure in CaC_6 is changed dramatically by introducing Ca atoms between graphene layers [27] exhibiting many unusual behaviors, such as charge density waves [28].

In this paper, we report the experimental observation of a linear-in-field quantum MR in CaC_6. A large nonsaturating MR of 244% is observed at 4 K under a magnetic field of 9 T. The B dependence of MR shows a linear behavior above 3 T and obeys a power law MR $\propto B^n$ with $n = 1.14$ in the whole field range (0–9 T) at 4 K. This behavior deviates apparently from a classical framework, where MR should follow a B^2 behavior, and points to the possible existence of an intrinsic linear Dirac-like fermion. This scenario is further confirmed qualitatively by performing first-principles band structure calculations. In addition, the possibility of disorder-related extrinsic origin of the observed linear MR is ruled out by comparing the data of the samples synthesized from highly oriented pyrolytic graphite and natural graphite. Those findings here may pave an avenue for study of the interplay between the linear Dirac-like and superconducting states.

II. EXPERIMENTS AND SAMPLE CHARACTERIZATION

Bulk CaC_6 samples are synthesized by the reaction between graphite and molten lithium-calcium alloy at about 400 °C for

*mugang@mail.sim.ac.cn
†liwei@mail.sim.ac.cn

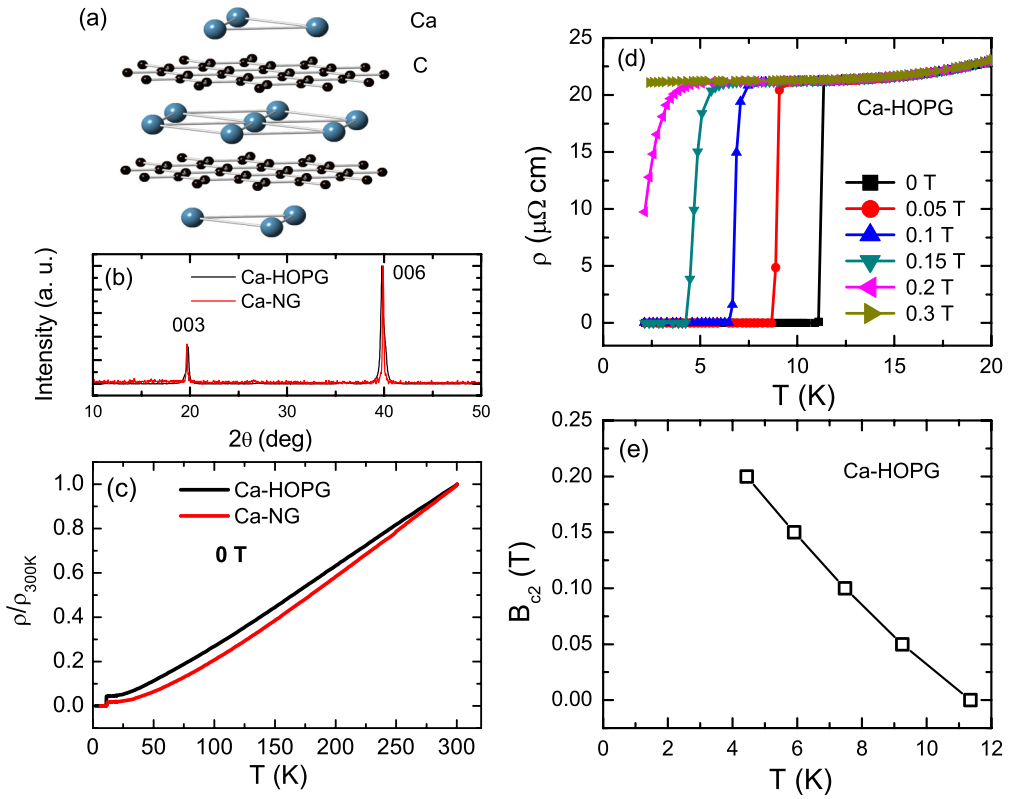

FIG. 1. (Color online) (a) The schematic crystal structure of CaC_6 and (b) the corresponding x-ray diffraction patterns for the Ca-HOPG and Ca-NG samples. Here, only peaks along the (00l) orientation are observed suggesting a high c-axis orientation. (c) Temperature dependence of resistivity up to 300 K under zero field for Ca-HOPG and Ca-NG samples. The data are normalized to the value of 300 K. A clear superconducting transition at $T_c = 11.4$ K can be seen. (d) The enlarged view of the resistivity data in the low-temperature region under different fields for the Ca-HOPG sample. (e) The B_{c2}-T phase diagram derived from the resistive transition curves in (d).

two weeks [25]. Both the highly oriented pyrolytic graphite (HOPG) and natural graphite (NG) are used for comparison. The lithium-calcium alloy is rich in lithium with a composition of Li:Ca=3:1. The reaction is performed in a stainless steel crucible under a protective argon atmosphere. Platelike samples with a silver color are obtained by exfoliating the surface layer stained by the alloy. The color of the sample surface becomes pale after exposing to air for several minutes, but the bulk properties remain unchanged after several days as revealed by x-ray diffraction and resistance measurements. The Ca-intercalated samples synthesized from HOPG and NG are abbreviated as Ca-HOPG and Ca-NG, respectively, hereafter. No lithium is found in the samples under the present synthesis condition. The samples for the resistance measurement have a typical dimension of $1.0 \times 0.6 \times 0.16\,\text{mm}^3$. The crystal structure is checked by x-ray diffraction (XRD) measurements at room temperature using a DX-2700 diffractometer with Cu K_α radiation. The electrical resistance is measured using a four-probe technique on a Quantum Design physical properties measurement system (PPMS) with magnetic field up to 9 T. The magnetic field is oriented parallel to the c axis of the samples.

As shown in Fig. 1(a), CaC_6 was reported to have a rhombohedral crystal structure with an $R\bar{3}m$ space group [29]. We examined the crystal structure of our samples by the XRD measurements. The XRD patterns for two samples Ca-HOPG and Ca-NG are shown in Fig. 1(b). It is clear that only peaks along the (00l) orientation can be observed, suggesting a high c-axis orientation. The interlayer distance between two graphene sheets is determined to be 4.503 ± 0.025 Å, which is consistent with the reports by other groups [24,25,29]. The full width at half maximum (FWHM) of the Ca-NG sample is clearly smaller than that of the Ca-HOPG sample, indicating a higher sample quality. The superconducting properties are checked by magnetization (data not shown here) and resistivity measurements. In Fig. 1(c), we show the temperature dependence of the in-plane electrical resistivity for the two samples up to 300 K. A sharp superconducting transition can be seen at low temperature. The critical transition temperature T_c is determined to be about 11.4 K, being very close to that reported in the literatures [24,25]. Above T_c, the ρ-T curve shows a metallic behavior. We can see that the Ca-NG sample has a larger residual resistance ratio (RRR $= R_{300K}/R_{0K}$) of 69, as compared with the Ca-HOPG sample (∼23). This is quite consistent with the XRD measurements as shown in Fig. 1(b), again suggesting a rather higher sample quality with a very low level of inhomogeneity and disorder for Ca-NG. By applying a magnetic field the transition shifts to lower temperatures quickly, as shown in Fig. 1(d) for the sample Ca-HOPG. The onset transition points under different fields are determined and presented in Fig. 1(e). We note that this B_{c2}-T phase diagram is quite consistent with that obtained from magnetization measurements [25].

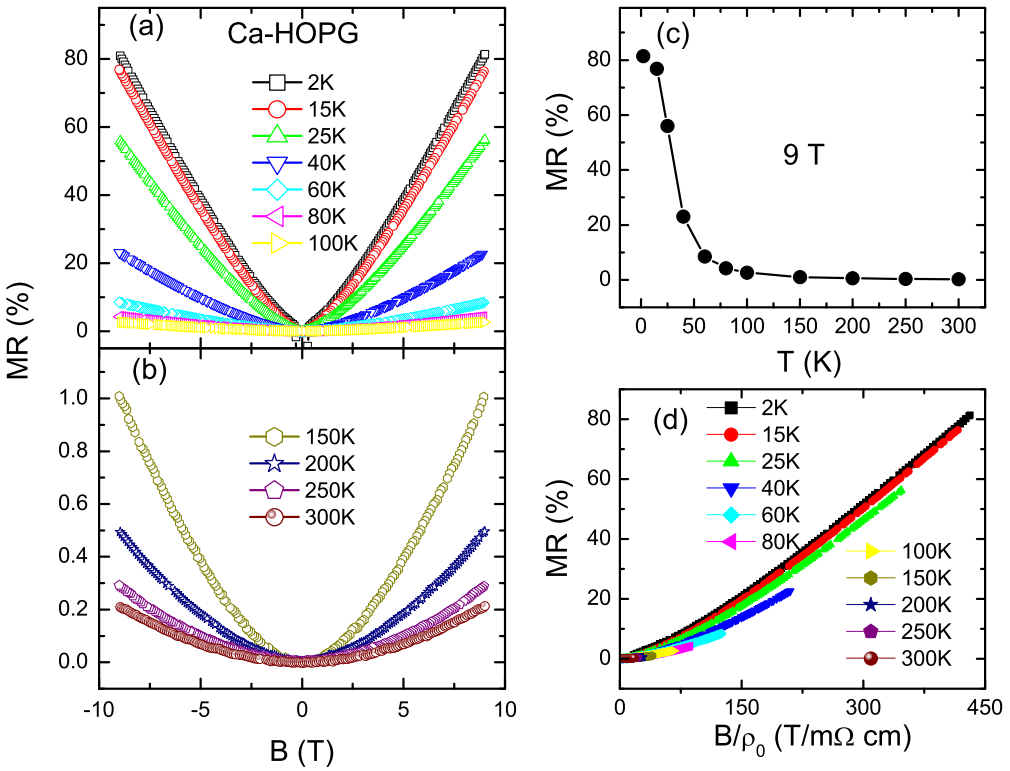

FIG. 2. (Color online) The MR data for the sample Ca-HOPG. (a) and (b) Field dependence of MR $= [\rho(B) - \rho_0]/\rho_0$ at different temperatures ranging from 2 K to 300 K, where ρ_0 is the resistivity under zero field. (c) Temperature dependence of MR obtained under 9 T. (d) The Kohler plot at different temperatures.

III. RESULTS AND DISCUSSION

The features on how magnetic fields influence electrons in a solid always reveal information about the electronic structure. Magnetoresistance is a very powerful tool to investigate this issue. Field dependence of MR at different temperatures for the sample Ca-HOPG is shown in Figs. 2(a) and 2(b). The data are measured for both positive and negative field orientations. Practically, the resistivity under field B is taken as $\rho(B) = [\rho(+B) + \rho(-B)]/2$ at each point to eliminate the effect of the Hall signals. Here MR is expressed as MR $= [\rho(B) - \rho(0)]/\rho(0)$. A quite large magnitude of MR ($\sim$81%) is observed at low temperature under 9 T, which decreases quickly with the increase of temperature as shown in Fig. 2(c). Interestingly, at low temperatures below 40 K the field-dependent MR clearly departs from the quadratic behavior expected classically [14]. Instead, it shows a nearly linear field dependence, especially in the high-field region. As the temperature increases, the MR evolves toward a classical quadratic field dependence. We also found that that Kohler's rule [30] based on the isotropic single-band scenario is violated, as shown in Fig. 2(d).

To have a comprehensive understanding, we quantified the field-dependent evolution by fitting the data in Fig. 2 with different functions. As shown in Fig. 3, the MR data at 15 K cannot be well fitted by the quadratic law ($\propto B^2$), which is the conventional MR behavior for metals in the low-B region, but can be described as a crossover behavior from B^2 to B with increasing B. In order to check the evolution with temperature, we also fitted the data at different temperatures using a power-law function MR $= A|B|^n$. As an example, the fitting curve at 15 K is represented by the green dashed line, which describes our data in the whole field range quite well. The obtained

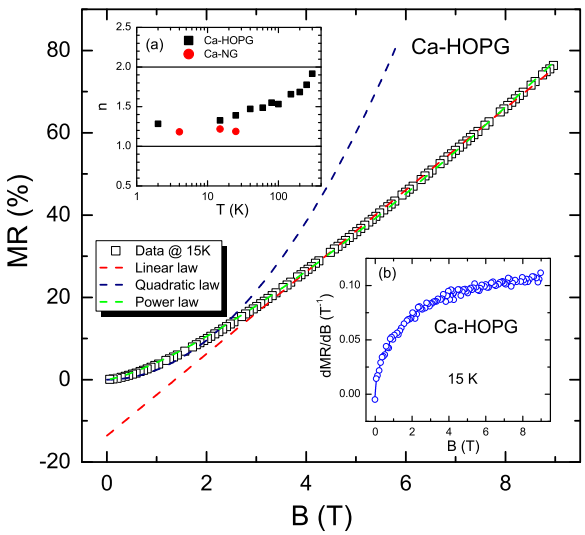

FIG. 3. (Color online) Field-dependent MR data for Ca-HOPG sample at 15 K and the fitting results based on linear law, quadratic law, and power law. Here we only show the data in the field range 0–9 T. Inset (a) shows the temperature dependence of the power exponent n from the power-law fittings. The results of sample Ca-NG are also displayed to have a comparison. Inset (b) shows the field derivative of MR at 15 K.

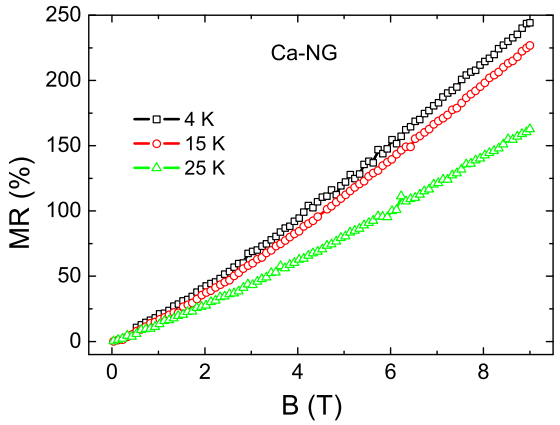

FIG. 4. (Color online) Field-dependent MR at 4 K, 15 K, and 25 K for the Ca-NG sample. The magnitude of MR can be as high as 244% at 4 K under 9 T.

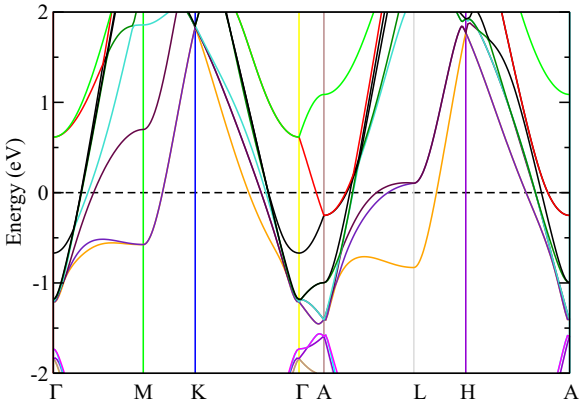

FIG. 5. (Color online) The band structure of CaC_6 obtained by the first-principles calculations. The Fermi energy is set to zero (black-dashed line).

power exponent n at different temperatures is shown in the inset (a) of Fig. 3, which increases monotonically from 1.28 at 2 K to 1.92 at 300 K showing an evolution from the linear to quadratic field dependence of MR. The linear behavior of MR at low temperatures is also confirmed by the field derivative of the data. As shown in the inset (b) of Fig. 3, the field derivative of MR ($d\mathrm{MR}/dB$) at 15 K increases quickly in the low-field region and becomes saturated when the field is higher than about 3 T.

Next, we turn to discuss the origin of the experimentally observed large linear MR behavior. To explain such a behavior, we first consider the extrinsic case, which is composed of the mobility fluctuation in inhomogeneous samples [19] and/or disorder-induced quantum interference effect [20,21] as mentioned in the introduction. For this purpose, we also investigated the MR of the Ca-NG sample with a much higher quality as revealed by the smaller FWHM and larger RRR. Surprisingly we observed a much larger MR value as high as 244% at 4 K under a magnetic field of 9 T (see Fig. 4). Nevertheless, the curves show a similar linear-in-field behavior compared with the Ca-HOPG sample. We also fitted the data with the power-law function $\mathrm{MR} = A|B|^n$. The obtained parameter n can be seen in the inset of Fig. 3, which shows a slightly smaller value and is comparable with the results from Ca-HOPG sample. Such behavior supplies strong evidence that the disorder is not the origin of the observed large linear MR behavior. On the contrary, it suppresses such a large and linear MR. Consequently, our observations point towards an intrinsic origin of the large linear MR in CaC_6.

In order to examine whether the Dirac-like states exist in the low energy dispersion of electronic band structure, we carried out first-principles calculations, which are performed by using the pseudopotential-based code VASP [31] within the Perdew-Burke-Ernzerhof [32] generalized gradient approximation. Throughout the theoretical calculations, a 500 eV cutoff in the plane wave expansion and a $12 \times 12 \times 8$ Gamma $\vec{k}$ grid are chosen to ensure the calculation with an accuracy of 10^{-5} eV. The crystal structural parameters are taken from the experimental values. The calculated electronic band structure is shown in Fig. 5. Although this result is consistent with previously reported calculations [27,33–35], we present it here to facilitate the following discussion concerning the existence of Dirac-like states. Due to the enlarged interlayer distance by intercalated Ca atoms, the states from each layer of graphite favor forming the linear massless Dirac-like band structure, similar to that of graphene but with double degeneracies. Due to the interlayer interaction between graphenes hybridized by the Ca s orbital, the linear massless Dirac-like dispersion will be broken making the band structure become a linear massive Dirac-like one (e.g., the yellow line between K and Γ points in Fig. 5), which has been observed experimentally by the angle-resolved photoelectron spectroscopy [36]. Qualitatively, according to the theory proposed by Abrikosov [15,16], the linearly dispersive band structures lead to a linear field dependence of MR at a low magnetic field. Therefore, we can argue that the experimentally observed linear MR in CaC_6 may be ascribed to an intrinsic mechanism of the presence of massive Dirac-like dispersion in the low-energy band structure. Furthermore, it is also interesting to point out that the multiband effect behaves in the transport process [35,37]. Intuitively, we expect that all the energy bands, including the ones with parabolic relation of dispersion, crossing the Fermi level will contribute to the transport process. However, the contribution to the transport properties from the parabolic bands is suppressed dramatically because of the lower mobility of the carriers, compared with that from the linear Dirac-like bands. We note that such a effect of mobility difference between the Dirac-like and parabolic bands is very significant. Experimentally, such a behavior has been observed and analyzed by Huynh *et al.* in the $BaFe_2As_2$ system [7], where a sharp decrease in the resistivity was observed at the spin-density wave (SDW) transition, even if almost all of the carriers are suppressed due to the appearance of the SDW order. Moreover, it is well known that materials with a free-electron-like Fermi surface and the usual parabolic-dispersion bands typically show a very small MR [9,14]. Thus, we can safely neglect the contribution of the parabolic bands to the observed large linear MR. Quantitatively, the Fermi velocity v_F of the Dirac band and the lower limit of magnetic field B for the linear MR at low temperature are evaluated to be 3.06×10^5 m/s and 3 T from the first-principles calculations and our experimental results, respectively. Based

on the extended Abrikosov theory [11,13,17,18], where a high Landau level is occupied, we estimate the N (=3906)th Landau level located on the Fermi level under the field of B in low temperature in terms of the conditions $E(N) < E_0$ and $E(N+1) > E_0$; $E_0 \sim 1.2$ eV is the position of the Dirac point on the Γ point below the Fermi level and $E(N) = v_F\sqrt{2N\hbar eB}$ describes the Nth Landau level [1]. Importantly, the Landau level spacing near the Fermi level is about $\Delta = E(N+1) - E(N) = 0.15$ meV indicating the linear MR can survive up to 2 K, which qualitatively explains the nature of our experimental observations that linear MR is present at low temperature. To further quantitatively confirm those scenarios, we should utilize the low-energy effective tight-binding model, such as the Wannier orbital model [38,39], fitting to the obtained energy band structure. Once obtaining this effective Hamiltonian, the MR can be evaluated easily by using the linear response approximation [40]. In detail, we left this issue to be addressed in future theoretical studies.

Finally, from the viewpoint of applications, the experimentally observed large quantum MR has potential applications, such as high-density data storage and magnetic sensors and actuators. On the other hand, it is worth pointing out that although the quantum MR found in superconductor CaC_6 is set up beyond the critical transition point of superconductivity, these findings may suggest an avenue for further exploring the coexistence and interplay between the linear Dirac-like and superconducting states.

IV. CONCLUSION

In conclusion, we have reported the experimental observation of a linear-in-field MR in the Ca-intercalated graphite superconductor CaC_6. A large nonsaturating MR of 244% is observed for the Ca-NG sample at 4 K under a magnetic field of 9 T. The magnetic field (B) dependence of MR shows a linear behavior above 3 T at low temperature, which is not expected from a classical framework, pointing to the nature of the existence of linear Dirac-like dispersion at low-energy band structure. This scenario is confirmed qualitatively by performing first-principles band structure calculations. The importance of the results may open a route to explore the coexistence and interplay between the linear Dirac-like and superconducting states in exotic materials in future studies.

ACKNOWLEDGMENTS

We thank R. B. Tao, C. S. Ting, Y. Chen, S. Q. Shen, F. Q. Huang, Z. Liu, and S. L. Yang for helpful discussions. This work is supported by the Knowledge Innovation Project of the Chinese Academy of Sciences (No. KJCX2-EW-W11), the Natural Science Foundation of China (No. 11204338, No. 11227902, and No. 11404359), and the "Strategic Priority Research Program (B)" of the Chinese Academy of Sciences (No. XDB04040300). W.L. and X.X. also gratefully acknowledge the financial sponsorship by Shanghai Yang-Fan Program (Grants No. 14YF1407100 and No. 14YF1407000).

[1] A. H. Castro Neto, F. Guinea, N. M. R. Peres, K. S. Novoselov, and A. K. Geim, Rev. Mod. Phys. **81**, 109 (2009).
[2] M. Z. Hasan and C. L. Kane, Rev. Mod. Phys. **82**, 3045 (2010).
[3] X.-L. Qi and S.-C. Zhang, Rev. Mod. Phys. **83**, 1057 (2011).
[4] X. Wan, A. M. Turner, A. Vishwanath, and S. Y. Savrasov, Phys. Rev. B **83**, 205101 (2011).
[5] G. Xu, H. Weng, Z. Wang, X. Dai, and Z. Fang, Phys. Rev. Lett. **107**, 186806 (2011).
[6] P. Richard, K. Nakayama, T. Sato, M. Neupane, Y.-M. Xu, J. H. Bowen, G. F. Chen, J. L. Luo, N. L. Wang, X. Dai, Z. Fang, H. Ding, and T. Takahashi, Phys. Rev. Lett. **104**, 137001 (2010).
[7] K. K. Huynh, Y. Tanabe, and K. Tanigaki, Phys. Rev. Lett. **106**, 217004 (2011).
[8] Y. Tanabe, K. K. Huynh, S. Heguri, G. Mu, T. Urata, J. Xu, R. Nouchi, N. Mitoma, and K. Tanigaki, Phys. Rev. B **84**, 100508(R) (2011).
[9] A. L. Friedman, J. L. Tedesco, P. M. Campbell, J. C. Culbertson, E. Aifer, F. K. Perkins, R. L. Myers-Ward, J. K. Hite, C. R. Eddy, Jr., G. G. Jernigan, and D. K. Gaskill, Nano Lett. **10**, 3962 (2010).
[10] X. Wang, Y. Du, S. Dou, and C. Zhang, Phys. Rev. Lett. **108**, 266806 (2012).
[11] W. Wang, Y. Du, G. Xu, X. Zhang, E. Liu, Z. Liu, Y. Shi, J. Chen, G. Wu, and X. Zhang, Sci. Rep. **3**, 2181 (2013).
[12] J. H. Chu, S. C. Riggs, M. Shapiro, J. Liu, C. R. Serero, D. Yi, M. Melissa, S. J. Suresha, C. Frontera, A. Vishwanath, X. Marti, I. R. Fisher, and R. Ramesh, arXiv:1309.4750.
[13] J. Feng, Y. Pang, D. Wu, Z. Wang, H. Weng, J. Li, X. Dai, Z. Fang, Y. Shi, and L. Lu, arXiv:1405.6611.
[14] A. A. Abrikosov, *Fundamentals of the Theory of Metals* (North-Holland, Amsterdam, 1988).
[15] A. A. Abrikosov, Sov. Phys. JETP **29**, 746 (1969).
[16] A. A. Abrikosov, Phys. Rev. B **58**, 2788 (1998).
[17] Hao Tang, Dong Liang, Richard L. J. Qiu, and Xuan P. A. Gao, ACS Nano **5**, 7510 (2011).
[18] C. M. Wang and X. L. Lei, Phys. Rev. B **86**, 035442 (2012).
[19] M. M. Parish and P. B. Littlewood, Nature (London) **426**, 162 (2003).
[20] A. Gerber, I. Kishon, I. Ya. Korenblit, O. Riss, A. Segal, M. Karpovski, and B. Raquet, Phys. Rev. Lett. **99**, 027201 (2007).
[21] Jingshi Hu and T. F. Rosenbaum, Nat. Mater. **7**, 697 (2008).
[22] C. W. J. Beenakker, Phys. Rev. Lett. **97**, 067007 (2006).
[23] N. B. Kopnin and E. B. Sonin, Phys. Rev. Lett. **100**, 246808 (2008).
[24] T. E. Waller, M. Ellerby, S. S. Saxena, R. P. Smith, and N. T. Skipper, Nat. Phys. **1**, 39 (2005).
[25] N. Emery, C. Hérold, M. d'Astuto, V. Garcia, Ch. Bellin, J. F. Marêché, P. Lagrange, and G. Loupias, Phys. Rev. Lett. **95**, 087003 (2005).
[26] J. S. Kim, L. Boeri, R. K. Kremer, and F. S. Razavi, Phys. Rev. B **74**, 214513 (2006).
[27] I. I. Mazin, L. Boeri, O. V. Dolgov, A. A. Golubov, G. B. Bachelet, M. Giantomassi, and O. K. Andersen, Physica C **460-462**, 116 (2007).
[28] K. C. Rahnejat, C. A. Howard, N. E. Shuttleworth, S. R. Schofield, K. lwaya, C. F. Hirjibehedin, Ch. Renner, G. Aeppli, and M. Ellerby, Nat. Commun. **2**, 558 (2011).

[29] N. Emery, C. Hérold, and P. Lagrange, J. Solid State Chem. **178**, 2947 (2005).
[30] J. M. Ziman, *Electrons and Phonons*, Classics Series (Oxford University Press, New York, 2001).
[31] G. Kresse and J. Furthmuller, Phys. Rev. B **54**, 11169 (1996).
[32] J. P. Perdew, K. Burke, and M. Ernzerhof, Phys. Rev. Lett. **77**, 3865 (1996).
[33] I. I. Mazin, Phys. Rev. Lett. **95**, 227001 (2005).
[34] M. Calandra and F. Mauri, Phys. Rev. Lett. **95**, 237002 (2005).
[35] G. Csányi, P. B. Littlewood, A. H. Nevidomskyy, C. J. Pickard, and B. D. Simons, Nat. Phys. **1**, 42 (2005).
[36] S.-L. Yang, J. A. Sobota, C. A. Howard, C. J. Pickard, M. Hashimoto, D. H. Lu, S.-K. Mo, P. S. Kirchmann, and Z.-X. Shen, Nat. Commun. **5**, 3493 (2014).
[37] K. Sugawara, T. Sato, and T. Takahashi, Nat. Phys. **5**, 40 (2009).
[38] W. Li, X.-Y. Wei, J.-X. Zhu, C. S. Ting, and Y. Chen, Phys. Rev. B **89**, 035101 (2014).
[39] W. Li, J. Zang, and Y. Jiang, Phys. Rev. B **84**, 033409 (2011).
[40] A. A. Abrikosov, L. P. Gorkov, and I. Ye. Dzyaloshinsky, *Quantum Field Theoretical Methods in Statistical Physics* (Pergamon, Oxford, 1965).